JOURNAL OF SOLID STATE CHEMISTRY 71, 296–304 (1987)

Energy Migration in a Two-Dimensional Eu^{3+} Compound: $EuMgAl_{11}O_{19}$

M. BUIJS* AND G. BLASSE

Solid State Department, Physical Laboratory, University of Utrecht, P.O. Box 80,000, 3508 TA Utrecht, The Netherlands

Received October 22, 1986

Energy-transfer processes in $EuMgAl_{11}O_{19}$, which has a two-dimensional Eu^{3+} sublattice, have been evaluated. The Eu^{3+} ion occupies at least four different sites, between which energy transfer occurs. Above 17 K energy migration occurs over the Eu^{3+} sublattice to quenching centers. The characteristics of this process can be explained using two-dimensional migration models. In the region up to 80 K the migration proved to be a two-site nonresonant two-phonon-assisted process. © 1987 Academic Press, Inc.

1. Introduction

The influence of structural peculiarities of a system on the dynamics of optical excitations in that system is of current interest. Much work has, for instance, been performed on energy migration in one- and two-dimensional systems, both theoretically (see Refs. (*1–6*) and Refs. therein) and experimentally (see Refs. (*7–10*) and Refs. therein). The effect of the dimensionality on energy migration in rare-earth compounds has been dealt with in our laboratory (*11–13*).

In this paper we report on our investigations on energy migration in $EuMgAl_{11}O_{19}$. The Eu^{3+} sublattice of this compound is two-dimensionally ordered: the Eu^{3+} ions are situated in planes perpendicular to the *c*-axis. This is illustrated in Fig. 1, which gives the unit cell of $EuMgAl_{11}O_{19}$. The structure is of the magnetoplumbite type ($PbFe_{12}O_{19}$) (*14, 15*), where Eu^{3+} substitutes for Pb^{2+}, and Mg^{2+} and Al^{3+} substitute for Fe^{3+}. The rare-earth ions lie in mirror planes which separate the spinel blocks. The separation between two neighboring Eu^{3+} ions in one plane is 5.6 Å, compared to 12 Å between two neighboring Eu^{3+} ions in different planes. In view of the distance dependence of the interaction responsible for energy transfer between two Eu^{3+} ions, one expects the energy migration to be confined to the Eu^{3+} planes. A comparable situation was encountered in $NaEuTiO_4$ (*16*), where the Eu^{3+}–Eu^{3+} separation is 3.7 Å in the plane and 10 Å between the planes. In this compound the energy migration in the Eu^{3+} sublattice was found to be two dimensional.

The energy migration was studied by performing luminescence measurements, using broad band, as well as laser site-selective excitation, and time-resolved spectroscopy on a powder sample of $EuMgAl_{11}O_{19}$.

2. Experimental

The experimental set-up is described in Refs. (*11, 16*). Measurements were made in

* To whom correspondence should be addressed.

0022-4596/87 $3.00

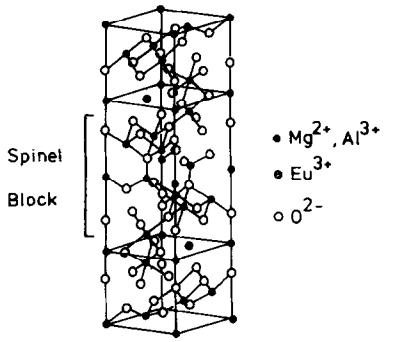

FIG. 1. Unit cell of $EuMgAl_{11}O_{19}$.

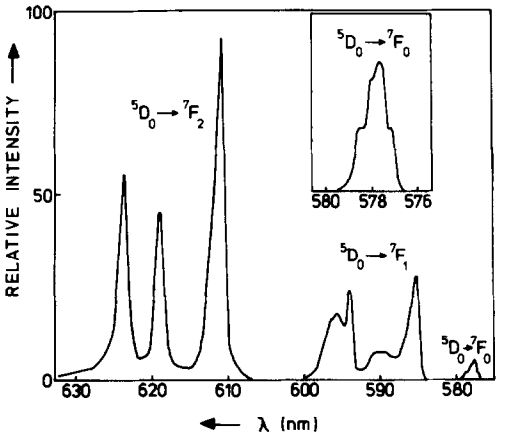

FIG. 2. Emission spectrum in the $^5D_0 \rightarrow {}^7F_{0,1,2}$ region of $EuMgAl_{11}O_{19}$, recorded at 1.3 K (λ_{exc} = 464.0 nm). Inset: magnification of the $^5D_0 \rightarrow {}^7F_0$ region.

the temperature region from 1.3 to 300 K.

The powder sample of composition $EuMgAl_{11}O_{19}$ was obtained from Prof. Dr. J. Liebertz, University of Cologne. It was prepared according to the description given in Ref. (*17*).

3. Results and Discussion

3.1. Spectral Properties

The excitation spectrum of the Eu^{3+} emission in $EuMgAl_{11}O_{19}$ consists of a broad band at 300 nm and several sharp lines in the region 350 to 600 nm. The broad band is ascribed to the O^{2-}–Eu^{3+} charge-transfer transition, while the sharp lines correspond to the well-known transitions within the $4f^6$ configuration of the Eu^{3+} ion.

The emission spectrum of $EuMgAl_{11}O_{19}$ in the $^5D_0 \rightarrow {}^7F_{0,1,2}$ region at 1.3 K under laser excitation into the $^7F_0 \rightarrow {}^5D_2$ transition at 464.0 nm is given in Fig. 2. The emission occurs from the $^5D_0$ level. The absence of emission from higher ^5D levels can be due to efficient multiphonon relaxation or to quenching by cross relaxation. The site symmetry of the Eu^{3+} ion was found to be C_{2v} in this compound (*18*). This lifts the selection rule which forbids the $^5D_0 \rightleftarrows {}^7F_0$ transition. Since levels with $J = 0$ are non-degenerate, the presence of four $^5D_0 \rightarrow {}^7F_0$ lines in Fig. 2 indicates that the Eu^{3+} ion occupies at least four different sites. This is probably due to the random distribution of the Mg^{2+} ions over the Fe^{3+} sites in the magnetoplumbite structure, which leads to a variety of possibilities for the cation surroundings of the Eu^{3+} ions. The positions of the four different $^5D_0 \rightleftarrows {}^7F_0$ transitions are given in Table I, together with the energy difference between the $^5D_0$ level and the $^7F_0$ level for every site.

These results are analogous to the ones obtained by Saber *et al.* (*18*), who performed luminescence measurements on $LaMgAl_{11}O_{19}:xEu^{3+}$ (x = 2%, 5%) at 77 and 300 K. These authors found two differ-

TABLE I

NUMERIC RESULTS OF THE Eu^{3+} $^5D_0 \rightleftarrows {}^7F_0$ TRANSITION IN $EuMgAl_{11}O_{19}$

Sites	λ (nm)	E^a (cm^{-1})
1	577.19	17325
2	577.75	17309
3	578.43	17288
4	578.92	17274

[a] The $^7F_0$ level is the ground level of the Eu^{3+} ion.

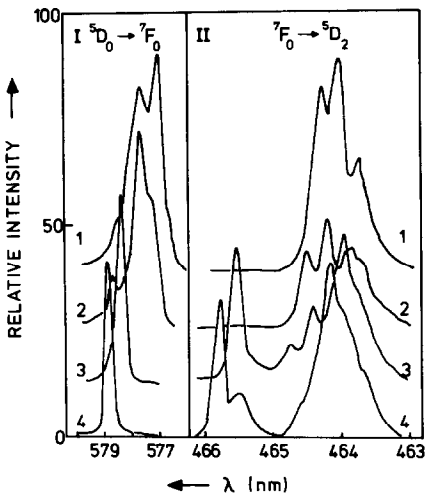

FIG. 3. Emission (I) and excitation (II) spectra of $EuMgAl_{11}O_{19}$ in the $^5D_0 \rightarrow {}^7F_0$ and $^7F_0 \rightarrow {}^5D_2$ regions, respectively, recorded at 4.2 K. I: λ_{exc} = 463.76 nm (1), 464.19 nm (2), 465.55 nm (3), and 465.78 nm (4); II: λ_{em} = 577.19 nm (1), 577.75 nm (2), 578.43 nm (3), and 578.92 nm (4).

ent sites for the Eu^{3+} ion, with $^5D_0 \rightarrow {}^7F_0$ transitions at 577.9 nm (A) and 578.6 nm (B) at 77 K.

For a further examination of these sites, excitation spectra of the different $^5D_0 \rightarrow {}^7F_0$ emission lines were recorded in the $^7F_0 \rightarrow {}^5D_2$ region at 4.2 K. These are shown in Fig. 3. The broad lines between 463 and 465 nm belong mainly to sites 1 and 2 as can be seen from Fig. 3 II, lines 1 and 2. The occurrence of these lines in the excitation spectra of sites 3 and 4 points to energy transfer from sites 1 and 2 to sites 3 and 4. Similarly, the shoulder at 465.6 nm in Fig. 3 II, line 4 points to energy transfer from site 3 to site 4. We will come to this below. Saber *et al.* (*18*) also found energy transfer from the Eu^{3+} (A) ion to the Eu^{3+} (B) ion at 77 K. At higher temperatures, site selection of the four different sites fails because of thermalization of the different $^5D_0$ levels.

3.2. Energy Transfer

The site-selective measurements presented in Fig. 3 indicate energy transfer between Eu^{3+} ions on different sites. We were able to confirm this with time-resolved measurements. In Fig. 4 is given the Eu^{3+} $^5D_0$ emission decay curve belonging to site 2 while exciting into the $^5D_2$ level of Eu^{3+} ions on site 1. The buildup with a rise time of about 100 μsec is due to energy transfer from a Eu^{3+} ion on site 1 to a Eu^{3+} ion on site 2.

The buildup is not due to relaxation from $^5D_2$ to $^5D_0$. This relaxation is too fast to be

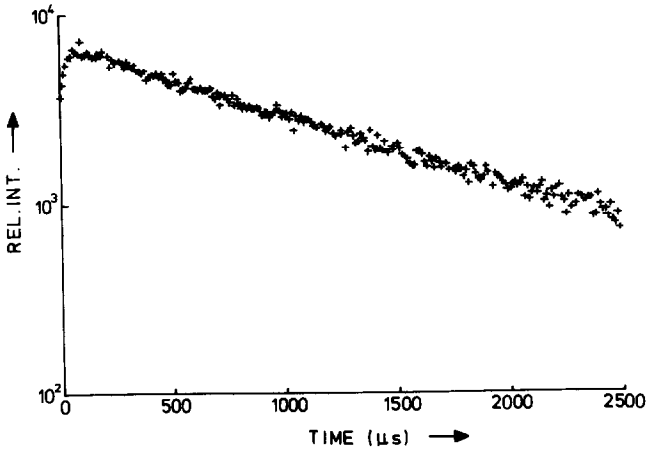

FIG. 4. Semilogarithmic decay curve of the $^5D_0$ emission (λ_{em} = 577.75 nm) of Eu^{3+} ions on site 2 in $EuMgAl_{11}O_{19}$ after excitation in the Eu^{3+} ions on site 1 (λ_{exc} = 463.76 nm), recorded at 4.2 K.

noticed on the time scale under consideration, since we do not see any emission from the $^5D_2$ or $^5D_1$ levels and since no buildup occurred in the $^5D_0$ emission decay curves of Eu^{3+} ions on one site after excitation into the $^5D_2$ level of the Eu^{3+} ions on the same site. In a similar way we found energy transfer to occur from 1 to 3 and 4, from 2 to 3 and 4, and from 3 to 4. The energy-transfer process can be denoted by

$$^5D_0(i) + {}^7F_0(j) \rightarrow {}^7F_0(i) + {}^5D_0(j), \quad (1)$$

where $1 \leq i \leq 3$, $2 \leq j \leq 4$, and $j < i$. Obviously the transfer at 4.2 K occurs downhill with respect to the positions of the $^5D_0$ levels, probably under emission of a phonon which matches the energy difference between the $^5D_0$ levels involved.

Besides the transfer between Eu^{3+} ions, there also exists energy migration on the Eu^{3+} sublattice in $EuMgAl_{11}O_{19}$. This is demonstrated in Fig. 5, which gives the integrated Eu^{3+} emission intensity ($^5D_0 \rightarrow {}^7F_{0,1,2}$) under broad band excitation into the $^7F_{0,1,2} \rightarrow {}^5L_6$ transition as a function of temperature. It shows that above 17 K a quenching of the intensity occurs, which is due to migration of the excitation energy to centers where it is lost nonradiatively. This phenomenon is usually encountered in concentrated Eu^{3+} compounds in which the Eu^{3+}–Eu^{3+} separation is not large enough

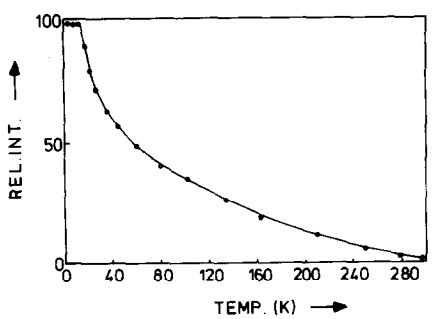

FIG. 5. Temperature dependence of the integrated Eu^{3+} ($^5D_0 \rightarrow {}^7F_{0,1,2}$) emission intensity of $EuMgAl_{11}O_{19}$ (λ_{exc} = 394 nm).

to prevent transfer (*11*, *16*). It can also be seen from Fig. 5 that the quenching rate increases with temperature. Comparison of the quantum efficiency of the $EuMgAl_{11}O_{19}$ sample at 300 K with the known quantum efficiency of a $EuMgB_5O_{10}$: 1% Nd^{3+} sample (*11*), which has a comparable luminescence intensity, leads to an efficiency of a few percent for the former, which is in agreement with Fig. 5, assuming that the quantum efficiency is 100% at 4.2 K. This is a reasonable assumption, since there is no energy migration at that temperature and nonradiative losses can be neglected.

The absence of energy migration at 4.2 K enables us to give a more quantitative description of the energy-transfer process between Eu^{3+} ions on different sites. The transfer takes place via the $^5D_0 \rightleftarrows {}^7F_0$ transition. Since this is a forced electric dipole transition and exchange interaction is very improbable for a Eu^{3+}–Eu^{3+} separation of 5.6 Å (*11*), it is reasonable to assume that the interaction responsible for the transfer is of a dipolar nature. We can then use the Inokuti–Hirayama formula to describe the decay of the donor intensity in the absence of backtransfer. It reads (*19*)

$$I(t) = I_0 \exp\left(-\frac{t}{\tau_0} - \pi^{1/2}\frac{N_a}{c_0}\left(\frac{t}{\tau_0}\right)^{1/2}\right), \quad (2)$$

where I_0 is the intensity at $t = 0$, τ_0 is the radiative decay time, N_a is the number of acceptor ions per unit volume, and c_0 is the critical transfer concentration, given by

$$c_0^{-1} = \tfrac{4}{3}\pi R_0^3, \quad (3)$$

and R_0 is the critical transfer distance for which the transfer rate is equal to the radiative decay rate.

From about 1500 μsec on, all the decay curves recorded at 4.2 K appeared to be exponential with a decay time of 1300 μsec. Since there is no energy migration at this temperature, this has to be equal to the

radiative decay time. The intersite Eu^{3+} transfer affects only the initial part of the decay curves. For an unambiguous analysis we used the decay curve of the Eu^{3+} $^5D_0$ emission belonging to site 3 after excitation into Eu^{3+} ions on site 3, which is given in Fig. 6. This donor has the advantage that it has only one type of acceptor ions, viz., Eu^{3+} ions on site 4. Their concentration was estimated from the ratio of the $^7F_0 \rightarrow {}^5D_0$ (site 4) intensity and the total $^7F_0 \rightarrow {}^5D_0$ intensity while monitoring the complete $^5D_0 \rightarrow {}^7F_2$ emission region, to be about 20% of the total Eu^{3+} concentration, which leads to a value for N_a of 5×10^{20} cm^{-3}. This estimation is done under the assumption that Eu^{3+} ions on different sites have equal absorption strength.

The decay of the Eu^{3+} ions on site 3 can be accurately described by Eq. (2). This is illustrated in Fig. 6, where the solid line gives the fit to Eq. (2). From the fit, the critical transfer distance can be derived to be about 6 Å for transfer from site 3 to site 4. This is in agreement with what one would have expected, namely, that the transfer is mainly restricted to nearest neighbors.

3.3. Energy Migration

The long-time part of the Eu^{3+} $^5D_0$ emission decay of the Eu^{3+} ions on all four sites is the same for all four sites for temperatures above 17 K. Examples of such curves are given in Figs. 7 and 8. They are nonexponential and decay at a faster rate than purely radiative. This reflects the fact that the excitation energy migrates over the Eu^{3+} sublattice to quenching centers. The decay rate increases in the temperature region from 17 to 150 K. Above 150 K it decreases slightly. The increase of the decay rate is due to an increase of the rate of migration, which is commonly observed in concentrated Eu^{3+} systems (*11*, *16*).

In view of the crystal structure one expects this energy migration to be two dimensional. Also, three-dimensional energy migration is experimentally ruled out because of the nonexponential long-time decay, which should be exponential for a three-dimensional migration process (*20*). Several expressions have been derived which describe the long-time behavior of the donor emission intensity in the case of

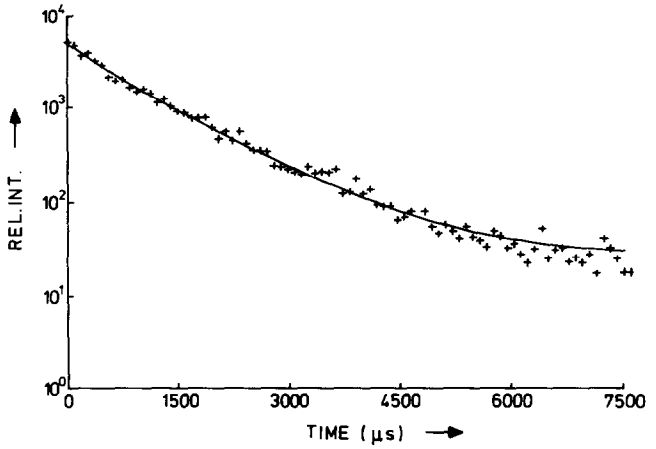

FIG. 6. Semilogarithmic decay curve of the $^5D_0$ emission (λ_{em} = 578.43 nm) of Eu^{3+} ions on site 3 in $EuMgAl_{11}O_{19}$ after excitation in the Eu^{3+} ions on site 3 (λ_{exc} = 465.55 nm), recorded at 4.2 K. Solid line: fit to Eq. (2).

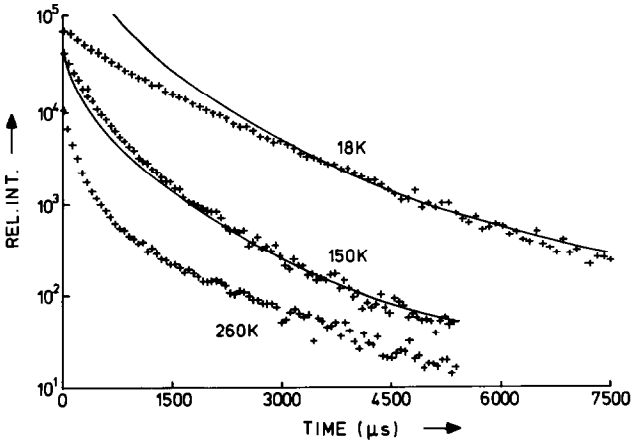

FIG. 7. Semilogarithmic decay curves of the Eu^{3+} $^5D_0$ emission (λ_{em} = 577.75 nm, λ_{exc} = 464.19 nm) in $EuMgAl_{11}O_{19}$, recorded at different temperatures. Solid lines: fits to Eq. (4).

two-dimensional energy migration over a donor sublattice to randomly distributed acceptors (quenching centers) in the absence of backtransfer. For the two-dimensional Eu^{3+} sublattice in $NaEuTiO_4$, the donor decay could be described within the framework of the average-t-matrix approximation (ATA) by using (*4, 20*).

$$I(t) = I_0 \exp\left(-\frac{t}{\tau_0}\right)(\alpha t)^{-1}, \qquad (4)$$

where the constant α depends on the concentration of acceptor ions x_a and the donor–donor transfer probability P. We tried to fit the long-time decay of the Eu^{3+} $^5D_0$ emission in the temperature region from 15 to 150 K to Eq. (4), with reasonable success, as is illustrated by the solid lines in Fig. 7. It has been stated, however, that the ATA method is not the most suitable method to describe energy migration in low-dimensional systems (*2, 21*). Numerical simulations (*5*) have shown that a better description in one- and two-dimensional systems can be given using the theory of

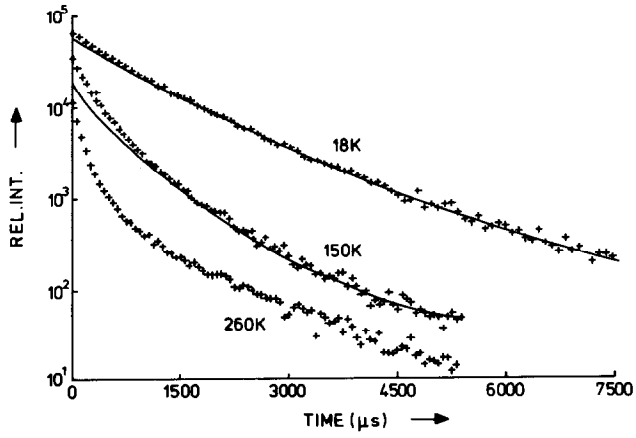

FIG. 8. Same as Fig. 7. Solid lines: fits to Eq. (5).

a random walk (RW) over the donor sublattice to randomly distributed acceptors which trap the migrating excitation at first encounter. This leads to a long-time behavior of the donor intensity of the form (*1*)

$$I(t) = I_0 \exp\left(-\frac{t}{\tau_0} - \beta t^{d/(d+2)}\right), \quad (5)$$

where the constant β depends on the acceptor concentration and the donor–donor transfer probability, and d is the dimensionality of the system. In the one-dimensional case Eq. (5) conforms with the exact solution of the deep-trap problem (*2*). We found that it represents a very good description of the Eu^{3+} decay in a one-dimensional concentrated Eu^{3+} compound, viz., $EuMgB_5O_{10}$ (*11*). In the two-dimensional Eu^{3+} compound studied here, Eq. (5) appeared also to describe the Eu^{3+} decay very well for long times after the excitation pulse in the temperature region from 17 to 150 K. The solid lines in Fig. 8 are two examples of fits to Eq. (5).

From the quality of the fits no conclusions can be drawn on the applicability of the two models leading to Eqs. (4) and (5). The evaluation of the fit parameters, however, shed some light on this equation. The increase in the rate of migration from 17 to 150 K is due to an enhanced donor–donor transfer probability. It arises from the fact that there is an energy mismatch between the $^5D_0$ levels of Eu^{3+} ions on different sites, and that small variations occur in the energy levels of Eu^{3+} ions on the same site due to random strains and defects. As a result of the latter, the emission lines are inhomogeneously broadened. For example, the linewidth of the $^5D_0 \rightleftarrows {}^7F_0$ transition for site 4 is 10 cm^{-1} at 4.2 K, which exceeds the homogeneous linewidth (less than 1 cm^{-1} (*22*)) considerably. The energy mismatch can be overcome by phonon assistance, which is a temperature-dependent process. The theory of the temperature dependence of the transfer probability between donor ions has been treated by Holstein *et al.* (*23*).

For the ATA the fit parameter α is given by (*4*)

$$\alpha = \pi x_a P_{ATA} \quad (6)$$

while in the RW approach β follows the Eq. (5)

$$\beta = 8.52 x_a^{1/2} P_{RW}^{1/2}. \quad (7)$$

Since we do not know the concentration of acceptor ions, it is difficult to obtain absolute values for the transfer probability. It is, however, very reasonable to assume that x_a is temperature independent, so that the temperature dependence of P will be equal to the temperature dependence of α and β^2, respectively. These are given in Fig. 9. From the possible temperature dependences given in Ref. (*23*), α could be best described by

$$\alpha = A + BT + CT^3, \quad (8)$$

where $A = 280\ sec^{-1}$, $B = 11\ sec^{-1}\ K^{-1}$, and $C = 4.5 \times 10^{-3}\ sec^{-1}\ K^{-3}$, and β^2 by

$$\beta^2 = DT^3, \quad (9)$$

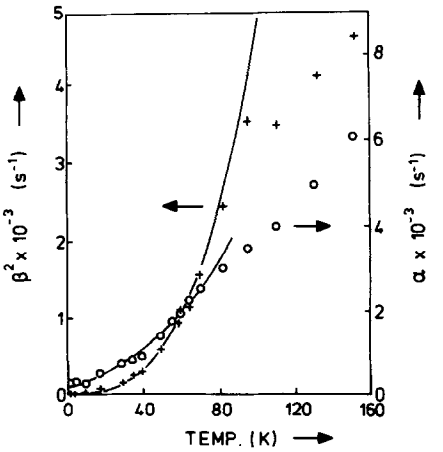

FIG. 9. Temperature dependence of α (circles) and β^2 (crosses). Solid lines: fits to Eqs. (8) and (9), respectively.

with $D = 6.0 \times 10^{-3}$ sec^{-1} K^{-3}, in the temperature region from 1.3 to 80 K. These equations are illustrated in Fig. 9 by the solid lines. The first two terms of Eq. (8) denote a direct one-phonon-assisted process, while the T^3 dependence is characteristic for a two-site nonresonant two-phonon-assisted process. The factors A, B, C, and D depend, among others, on the matrix element for the donor–donor interaction and the difference in ion–phonon coupling strength between the ground and excited state for the Eu^{3+} ions involved. These cannot be evaluated since no further data are available on $EuMgAl_{11}O_{19}$.

The two-phonon-assisted process is commonly encountered in rare-earth compounds. We found it to occur in $EuMgB_5O_{10}$ and $Gd_2(MoO_4)_3:Eu^{3+}$ (*11*, *24*), while Hamilton *et al.* (25) observed it in $LaF_3:Pr^{3+}$. Except for very low temperatures, below 10 K, where the transfer probability is only slightly dependent on temperature (*26*) (given by A in Eq. (8)), the direct one-phonon-assisted process proportional to T is seldom observed in rare-earth compounds. It is theoretically ruled out due to the fact that B is proportional to a coherence factor which becomes vanishingly small for interaction between similar sites with small energy mismatch (*23*), as is the case in $EuMgAl_{11}O_{19}$. The fact that we find, nevertheless, such a process if we apply the ATA method indicates that this method is inferior to the RW method for the description of the two-dimensional energy migration in this compound.

An estimation of the acceptor concentration can be made using the critical transfer distance R_0 of 6 Å between a Eu^{3+} ion on site 3 and a Eu^{3+} ion in site 4 at 4.2 K. From the definition of R_0 it can be derived that for dipole–dipole interaction the transfer probability depends on R_0 as

$$P_{\tau_0} = \left(\frac{R_0}{R}\right)^6, \qquad (10)$$

where R is the separation of the Eu^{3+} ions between which the transfer occurs. For nearest-neighbor Eu^{3+} ions ($R = 5.6$ Å) $R_0 = 6$ Å indicates that P is of the same order of magnitude as the radiative decay rate ($= \tau_0^{-1}$) at 4.2 K, viz., 10^3 sec^{-1}. If we assume that this value is representative for all the possible transfer probabilities between the different Eu^{3+} ions at 4.2 K, we can use it as the donor–donor transfer probability in the migration process if we extrapolate it to higher temperatures, using the T^3 dependence. The acceptor concentration can then be calculated, using Eq. (7), to be about 10^{-5} from

$$x_a = \frac{\beta^2}{8.52^2 \times 10^3 (T/4.2)^3}. \qquad (11)$$

The nature of the acceptor remains difficult to reveal. The diffuse reflectance spectrum of the $EuMgAl_{11}O_{19}$ powder shows a weak absorption band in the region of 400 to 600 nm. Since this overlaps with some of the emission lines of Eu^{3+} it can belong to the acceptors. This band might be related to the presence of Eu^{2+} as was suggested by Saber *et al.* (*18*).

Finally it should be pointed out that the slight decrease of the rate of migration above 150 K is contrary to what we found earlier in concentrated Eu^{3+} compounds (*11*, *24*). This might partly be due to the fact that at higher temperatures energy migration between Eu^{3+} ions in different planes is likely to occur. The probability of this process is $(5.6/12)^6 \approx 10^{-2}$ times the probability of the intraplane transfer probability for dipolar interaction. If we use the estimations of P and x_a derived above, it can be concluded that this interplane transfer probability at 80 K is of the same order of magnitude as the radiative decay probability, which means that three-dimensional migration also has to be taken into account. This so-called quasi-two-dimensional migration is sustained by the fact that the decay

curves tend to become exponential after long times at high temperatures, which is what one expects for this type of migration (*27*). Huber (*3*) has derived that the effective donor–donor transfer probability for quasi-two-dimensional migration is smaller than the probability for the two-dimensional case. This would, however, only explain a slowing down of the increase of the transfer probability with temperature, but not the slight decrease. It cannot be excluded that some temperature dependence of the donor–acceptor interaction is responsible for this.

In conclusion we can say that the layered structure of the Eu^{3+} lattice in $EuMgAl_{11}O_{19}$ can be recognized in the behavior of the energy migration which occurs above 17 K. The theory of phonon assistance for this process indicates that the average-*t*-matrix approximation leads to less satisfactory results in describing the migration than the random walk approach, which is in agreement with earlier numeric simulations. The analysis illustrates that the Eu^{3+} ion is a very versatile tool in the investigations on phonon-assisted energy-transfer processes due to the vast amount of different types of lattices in which this ion occurs and to the accessibility of its spectral properties.

Acknowledgments

We thank Prof. Dr. J. Liebertz for making the $EuMgAl_{11}O_{19}$ sample available. The investigations were supported by the Netherlands Foundation for Chemical Research (SON) with financial aid from the Netherlands Organization for Advancement of Pure Research (ZWO).

References

1. J. KLAFTER, G. ZUMOFEN, AND A. BLUMEN, *J. Physique Lett.* **45,** 49 (1984).
2. B. MOVAGHAR, G. W. SAUER, AND D. WÜRTZ, *J. Stat. Phys.* **27,** 473 (1982).
3. D. L. HUBER, *Phys. Rev. B* **26,** 3937 (1982).
4. K. K. GHOSH AND D. L. HUBER, *J. Lumin.* **21,** 225 (1980).
5. P. GRASSBERGER AND I. PROCACCIA, *J. Chem. Phys.* **77,** 6281 (1982).
6. R. D. WIETING, M. D. FAYER, AND D. D. DLOTT, *J. Chem. Phys.* **69,** 1996 (1978).
7. R. A. AUERBACH AND G. L. MCPHERSON, *Phys. Rev. B* **33,** 6815 (1986).
8. H. YAMAMATO, D. S. MCCLURE, G. MARZACCO, AND M. WALDMAN, *Chem. Phys.* **22,** 79 (1977).
9. R. M. SHELBY, A. H. ZEWAIL, AND C. B. HARRIS, *J. Chem. Phys.* **64,** 3192 (1976).
10. D. D. DLOTT, M. D. FAYER, AND R. D. WIETING, *J. Chem. Phys.* **69,** 2752 (1978).
11. M. BUIJS AND G. BLASSE, *J. Lumin.* **34,** 263 (1986).
12. M. BUIJS, J. P. M. VAN VLIET, AND G. BLASSE, *J. Lumin.* **35,** 213 (1986).
13. P. A. M. BERDOWSKI, M. BUIJS, AND G. BLASSE, *J. Phys. C* **7,** 31 (1985).
14. G. BLASSE AND A. BRIL, *Philips Res. Rep.* **21,** 368 (1966).
15. J. M. P. J. VERSTEGEN, J. L. SOMMERDIJK, AND J. G. VERRIET, *J. Lumin.* **6,** 425 (1973).
16. P. A. M. BERDOWSKI AND G. BLASSE, *J. Lumin.* **29,** 243 (1984).
17. J. LIEBERTZ, *Z. Kristallogr.* **166,** 297 (1984).
18. D. SABER, J. DEXPERT-GHYS, P. CARO, A. M. LEJUS, AND D. VIVIEN, *J. Chem. Phys.* **85,** 5648 (1985).
19. M. INOKUTI AND F. HIRAYAMA, *J. Chem. Phys.* **43,** 1978 (1965).
20. D. L. HUBER, *in* "Laser Spectroscopy of Solids" (W. M. Yen and P. M. Selzer, Eds.), Chap. 3. Springer, Berlin (1981).
21. B. MOVAGHAR, G. W. SAUER, D. WÜRTZ, AND D. L. HUBER, *Solid State Commun.* **39,** 1179 (1981).
22. G. BOULON, M. BOUDERBALA, AND J. SÉRIOT, *J. Less. Common Met.* **112,** 41 (1985).
23. T. HOLSTEIN, S. K. LYO, AND R. ORBACH, *in* "Laser Spectroscopy of Solids (W. M. Yen and P. M. Selzer, Eds.), Chap. 2. Springer, Berlin (1981).
24. M. BUIJS, G. BLASSE, AND L. H. BRIXNER, *Phys. Rev. B* **34,** 8815 (1986).
25. D. S. HAMILTON, P. M. SELZER, AND W. M. YEN, *Phys. Rev. B* **16,** 1858 (1977).
26. J. R. WIETFELD, D. S. MOORE, B. M. TISSUE, AND J. C. WRIGHT, *Phys. Rev. B* **33,** 5788 (1986).
27. P. A. M. BERDOWSKI, J. VAN HERK, AND G. BLASSE, *J. Lumin.* **34,** 9 (1985).